Supporting Information For

Rapid Switch-On Fluorescent Detection of Nanomolar Level Hydrazine in Water by a Diacetoxy Functionalized MOF: Application in Paper Strips and Environmental Samples

*Soutick Nandi, Mostakim SK, and Shyam Biswas**

Department of Chemistry, Indian Institute of Technology Guwahati, Guwahati, 781039 Assam, India

* Corresponding author. Tel: 91-3612583309, Fax: 91-3612582349.

E-mail address: sbiswas@iitg.ac.in

Materials and Characterization Methods. The ligand 2,5-diacetoxy terephthalic acid (H_2BDC-$(OCOCH_3)_2$) was achieved by following the previously reported procedure (Scheme S1).[1] A drastic naked eye color change was visualized during the product formation. 2,5-dihydroxyterephthalic acid (H_2BDC-$(OH)_2$) was bright yellow solid which was transformed to white solid compound when it was converted to 2,5-diacetoxy terephthalic acid (Figure S1). The ^1H NMR and ^{13}C NMR spectra of this ligand are shown in Figures S2-S3. All other required chemicals were purchased from commercial sources and used without purification. Fourier transform infrared (FT-IR) spectra were recorded with a Perkin Elmer Spectrum two FT-IR spectrometer in the range of 440-4000 cm^{-1} with KBr pellet. The below mentioned indications were employed for the characterization of the absorption bands: medium (m), weak (w), broad (br), very strong (vs), strong (s) and shoulder (sh). Ambient temperature X-Ray powder diffraction (XRPD) patterns were collected on a Bruker D2 Phaser X-ray diffractometer (30 kV, 10 mA) using Cu-$K\alpha$ (λ = 1.5406 Å) radiation. Lattice parameters were determined by using the DICVOL program[2] and refined by employing STOE's WinXPow software package.[3] FE-SEM images were captured with a Zeiss (Zemini) scanning electron microscope. Thermogravimetric analyses (TGA) were collected under air atmosphere at a heating rate of 10 °C min^{-1} in a temperature region of 25-800 °C by employing a Netzsch STA-409CD thermal analyzer. Fluorescence emission behavior was recorded by a HORIBA JOBIN YVON Fluoromax-4 spectrofluorometer. The excitation wavelength (λ_{ex}) was 365 nm for all the fluorescence experiments. The nitrogen sorption isotherms were performed employing a Quantachrome Autosorb iQ-MP gas sorption analyzer at -196 °C. Prior to the sorption measurement, degassing of the material was performed at 90 °C for 12 h under dynamic vacuum. A Bruker Avance III 600 spectrometer was utilized for recording ^1H NMR at 400 MHz. Fluorescence lifetime measurements were performed by time correlated single-photon counting (TCSPC) method by an Edinburgh Instrument Life-Spec II instrument. The fluorescence decays were analyzed by reconvolution method using the FAST software provided by Edinburgh Instruments.

Fluorescence Detection Assay in Aqueous Medium. The probe (5 mg) was taken in a glass vial in mili-Q water (5 mL) was included. The suspension was sonicated for 1 h. A stable suspension was obtained after keeping for overnight at static condition. The above-mentioned suspension (200 μL) of the probe was added inside a quartz cuvette. Then, we have included 2800 μL of mili-Q water to the suspension. All the fluorescence titration measurements were conducted by exciting the resulting suspension at 365 nm and recording the spectra within 385-710 nm. For time dependent fluorescence experiment, 500 μL of 1 mM hydrazine (NH_2NH_2) was introduced to the suspension of **1′** and in each minute, emission spectra were collected. To perform the concentration-dependent sensing event, 0 to 500 μL of hydrazine (1 mM) solution was added gradually to aqueous suspension of **1′**. After each addition, the emission response of the resulting suspension was observed. To ensure the specificity of the compound towards hydrazine detection event was performed with several possible interfering analytes. 1 mM solution of different compositing analytes have been prepared by dissolving required amounts of compounds in 5 mL mili-Q water (i.e. NaF, NaBr, NaCl, NaI, $NaNO_3$, $NaNO_2$, NaCN, NaN_3,

NaSCN, $NaHCO_3$, Na_2SO_4, Na_2SO_3, $NaHSO_3$, $NaHSO_4$, NaOAc, $NaClO_4$, NH_2OH, cysteine, aspartic acid, glucose, aspartic acid, serine and thiourea).

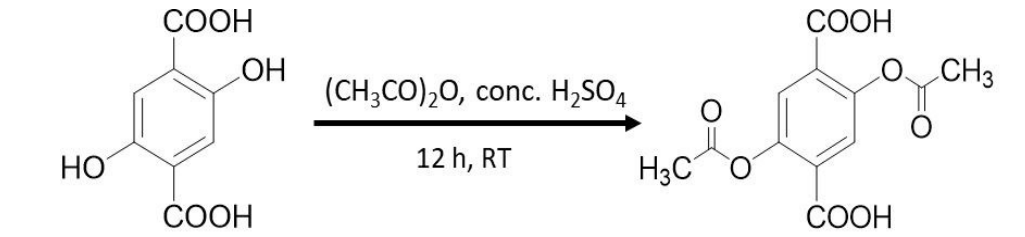

2,5-dihydroxyterephthalic acid
$H_2BDC-(OH)_2$

2,5-diacetoxyterephthalic acid
$H_2BDC-(OCOCH_3)_2$

Scheme S1. Scheme for the preparation of 2,5-diacetoxy terephthalic acid ($H_2BDC-(OCOCH_3)_2$).

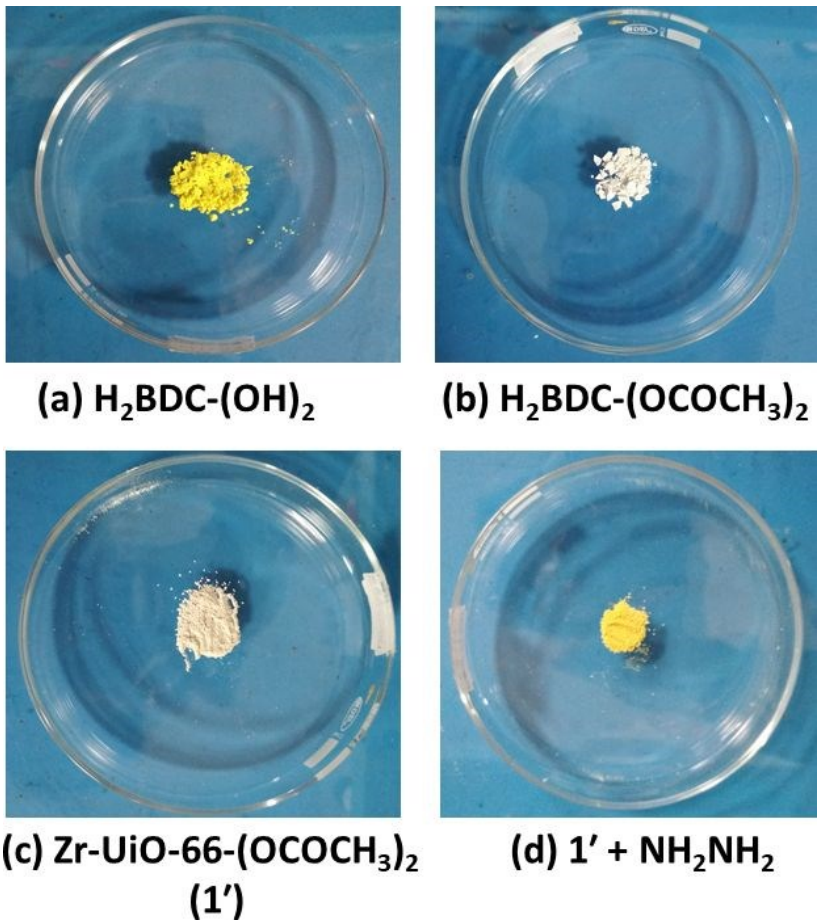

Figure S1. Photographs of (a) $H_2BDC-(OH)_2$ ligand, (b) $H_2BDC-(OCOCH_3)_2$ ligand, (c) Zr-UiO-66-$(OCOCH_3)_2$ MOF (**1′**) and (d) hydrazine treated **1′** (in bulk scale) under day light.

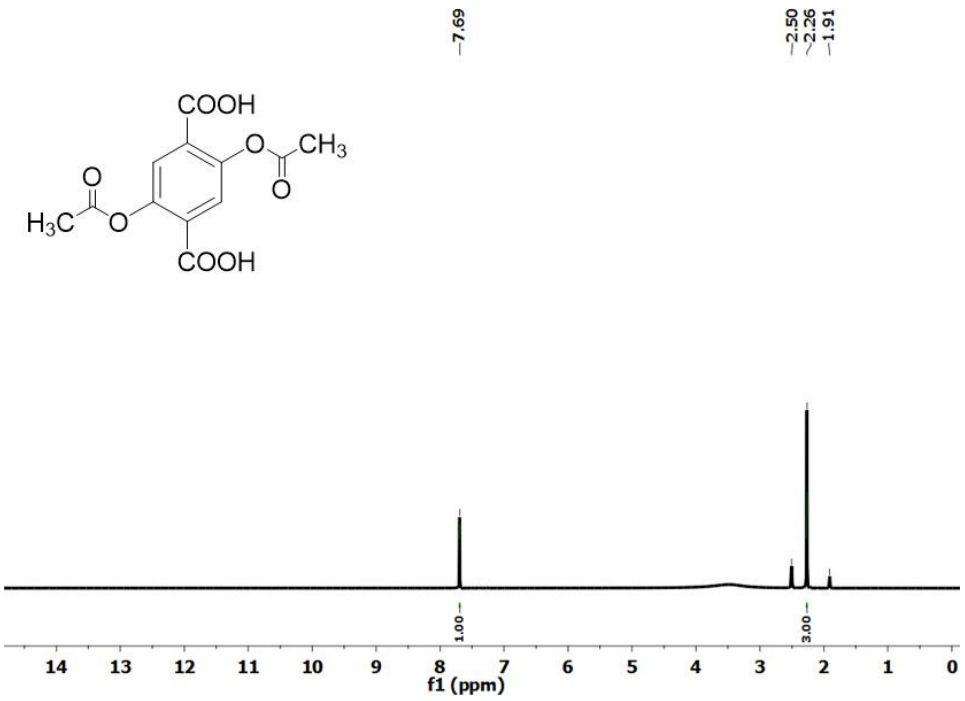

Figure S2. ^{1}H NMR spectrum of $H_2BDC\text{-}(OCOCH_3)_2$ ligand.

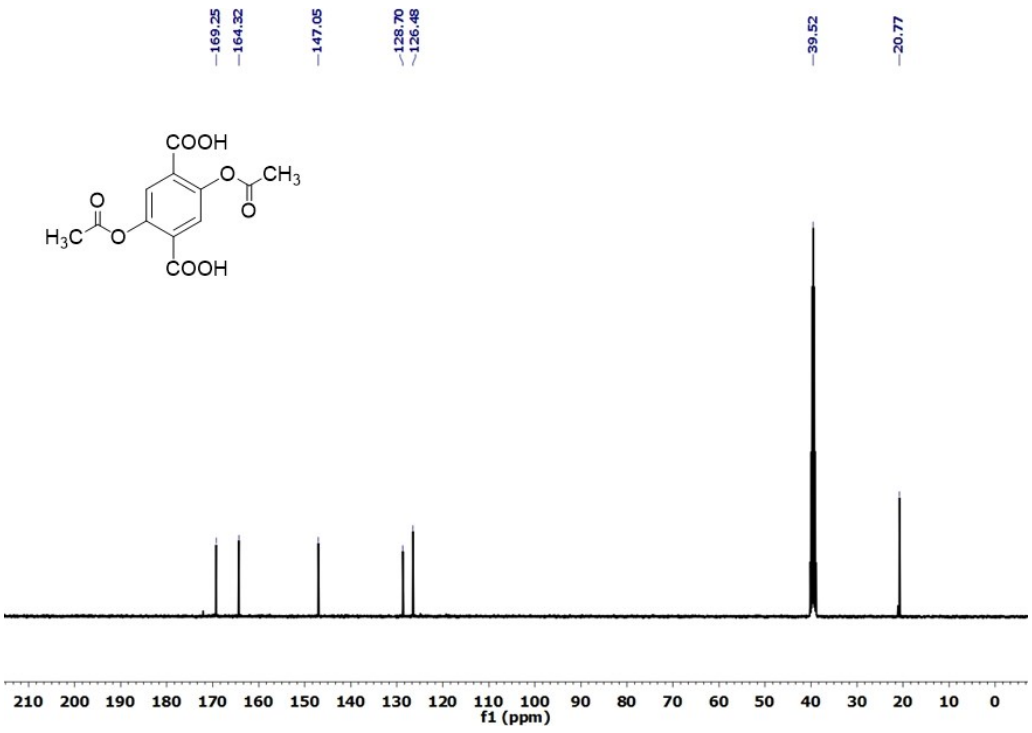

Figure S3. ^{13}C NMR spectrum of $H_2BDC\text{-}(OCOCH_3)_2$ ligand.

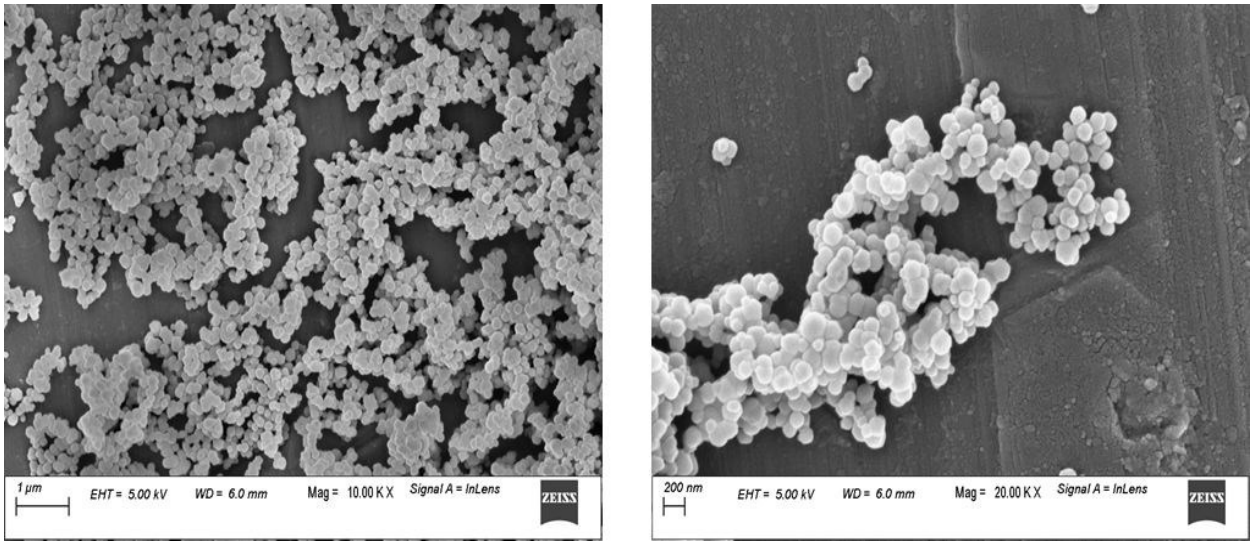

Figure S4. FE-SEM images of **1'** under different magnifications.

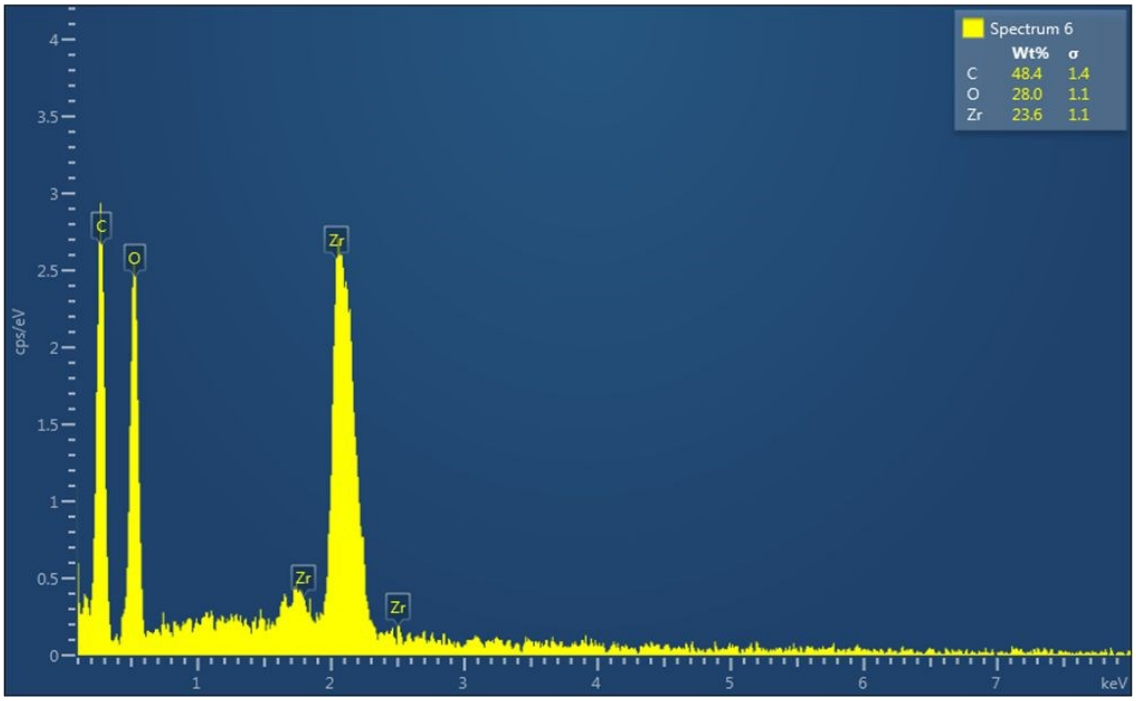

Figure S5. EDX spectrum of **1'**.

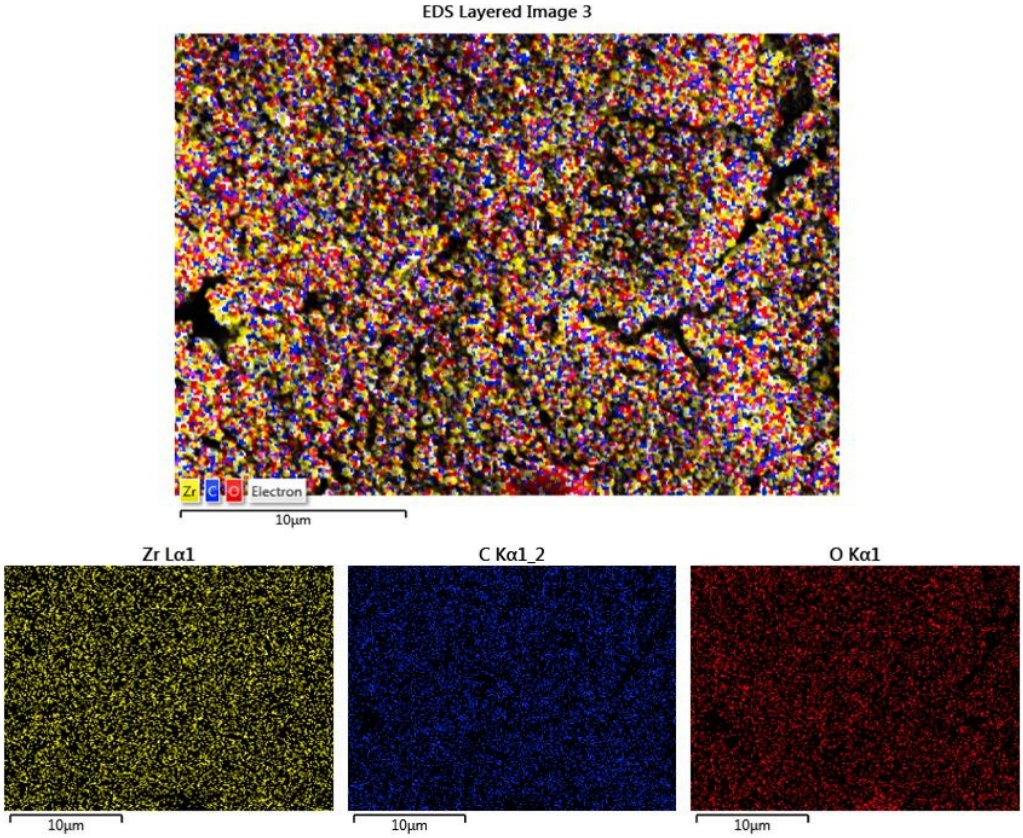

Figure S6. EDX elemental mapping of **1'**.

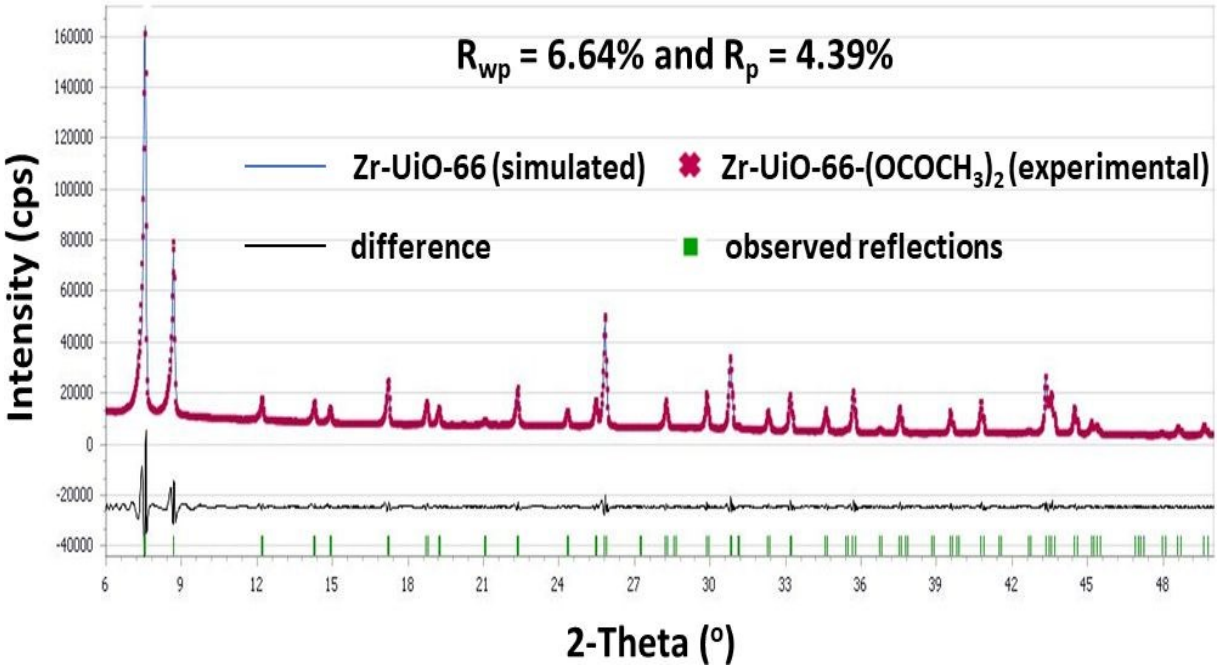

Figure S7. Pawley refinement for the XRPD pattern of as-synthesized **1**. Pink characters and blues lines denote experimental and simulated patterns, respectively. The peak positions and difference plot are displayed at the bottom (R_{wp} = 6.64%, R_p = 4.39%).

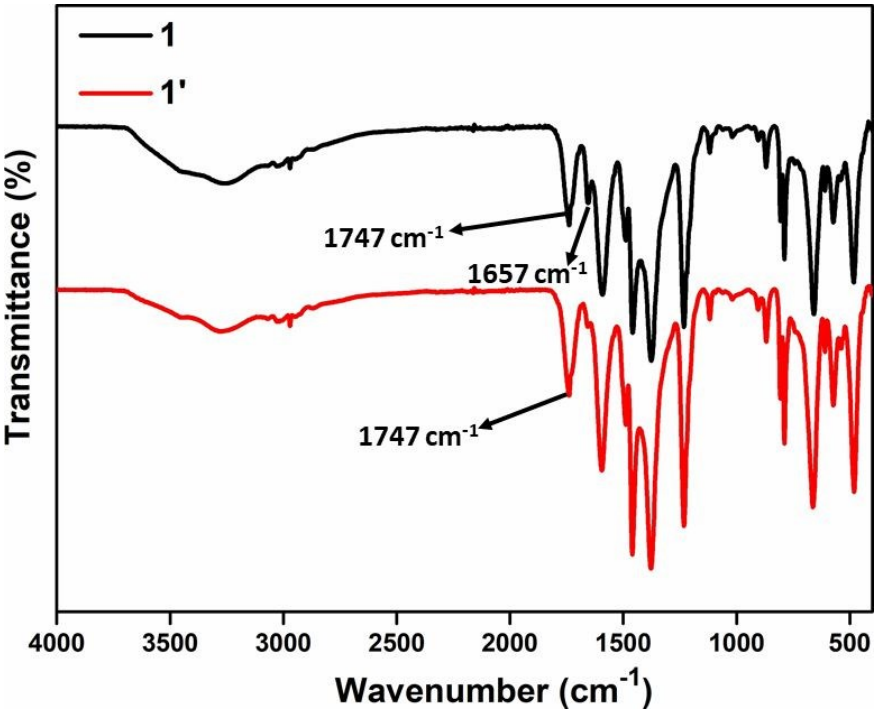

Figure S8. FT-IR spectra of as-synthesized **1** and thermally activated **1′**.

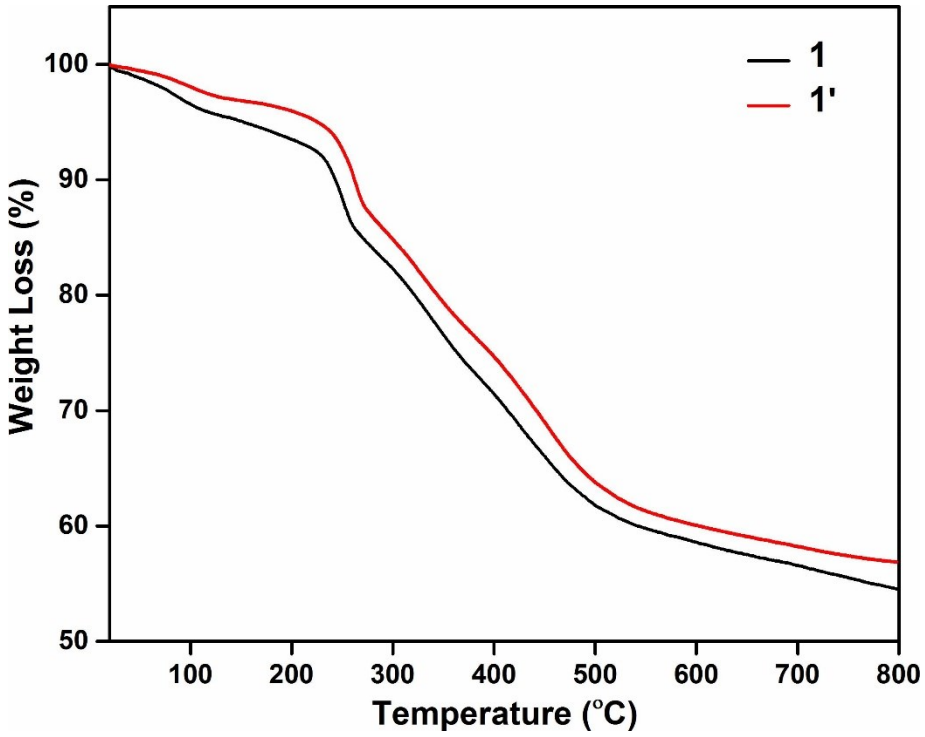

Figure S9. TG curves of as-synthesized **1** and activated **1′** measured in the temperature range of 25-700 °C at a heating rate of 10 ºC min^{-1}.

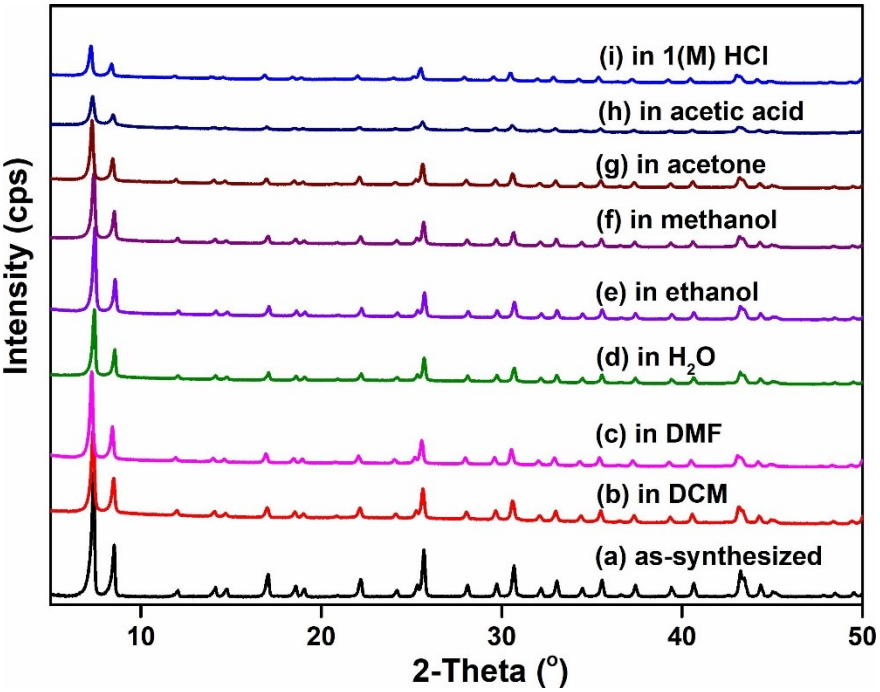

Figure S10. Experimental XRPD patterns of as-synthesized **1** (a), in DCM (b), in DMF (c), in water (d), in ethanol (e), in methanol (f), in acetone (g), in acetic acid (h) and in 1 (M) HCl (i).

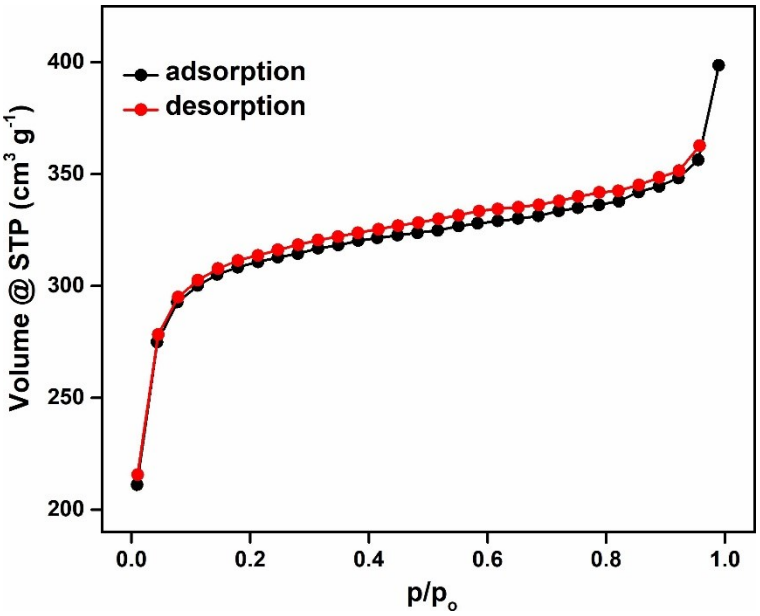

Figure S11. N_2 adsorption (solid black circles) and desorption (solid red circles) isotherms of **1′** measured at -196 °C.

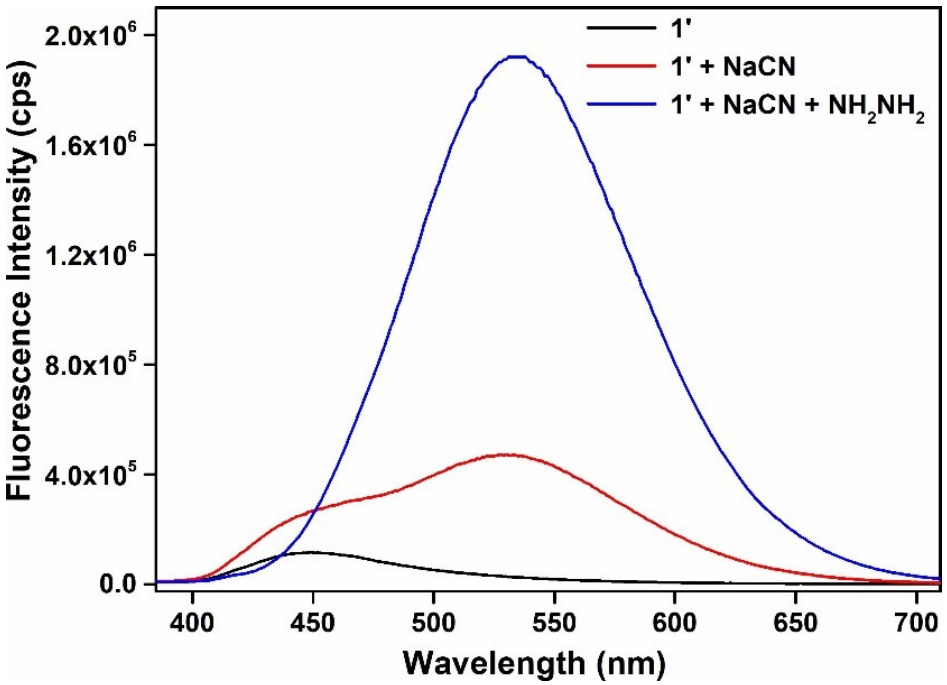

Figure S12. Change in the fluorescence emission intensity of **1′** upon addition of 1 mM hydrazine solution (500 µL) in presence of 1 mM NaCN solution (500 µL).

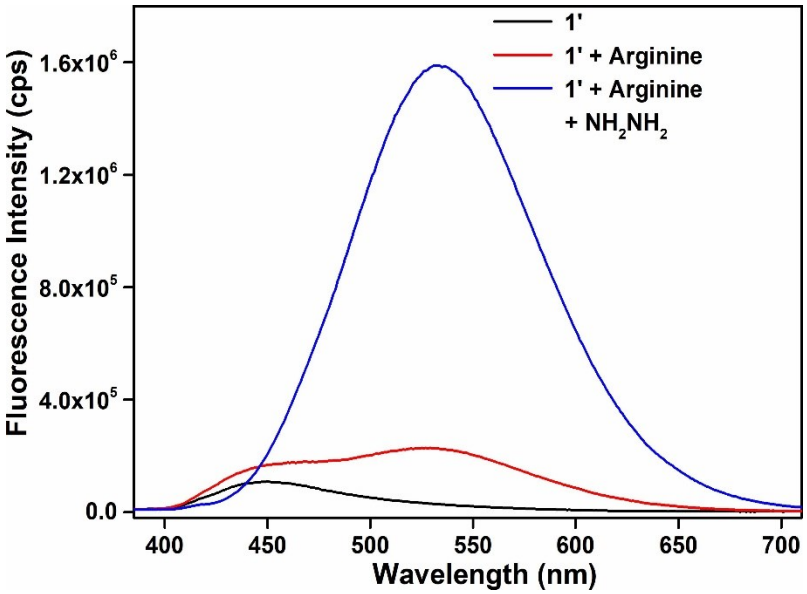

Figure S13. Change in the fluorescence emission intensity of **1′** upon addition of 1 mM hydrazine solution (500 µL) in presence of 1 mM arginine solution (500 µL).

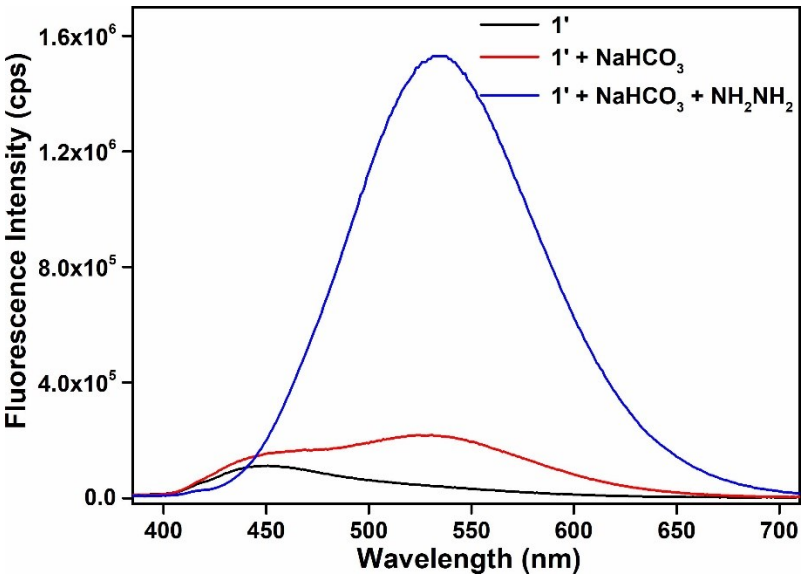

Figure S14. Change in the fluorescence emission intensity of **1′** upon addition of 1 mM hydrazine solution (500 µL) in presence of 1 mM $NaHCO_3$ solution (500 µL).

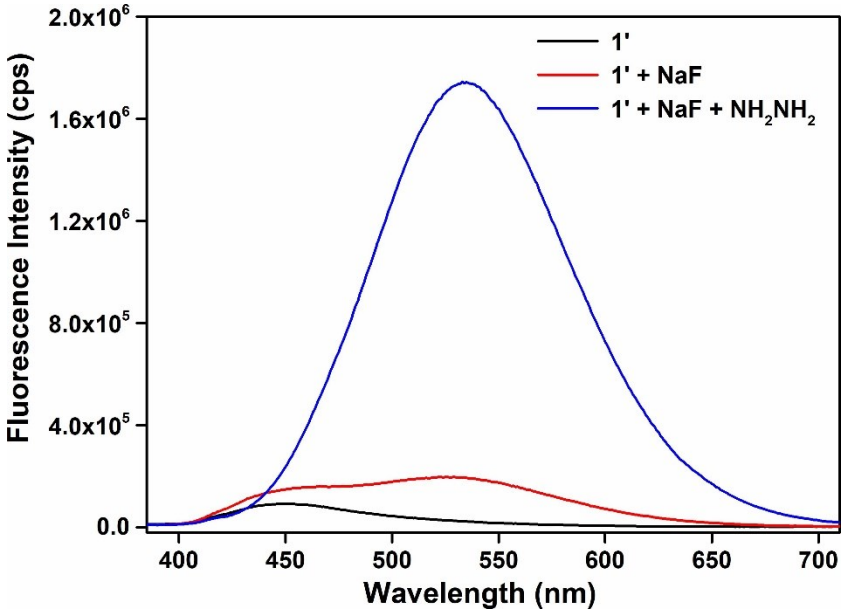

Figure S15. Change in the fluorescence emission intensity of **1′** upon addition of 1 mM hydrazine solution (500 µL) in presence of 1 mM NaF solution (500 µL).

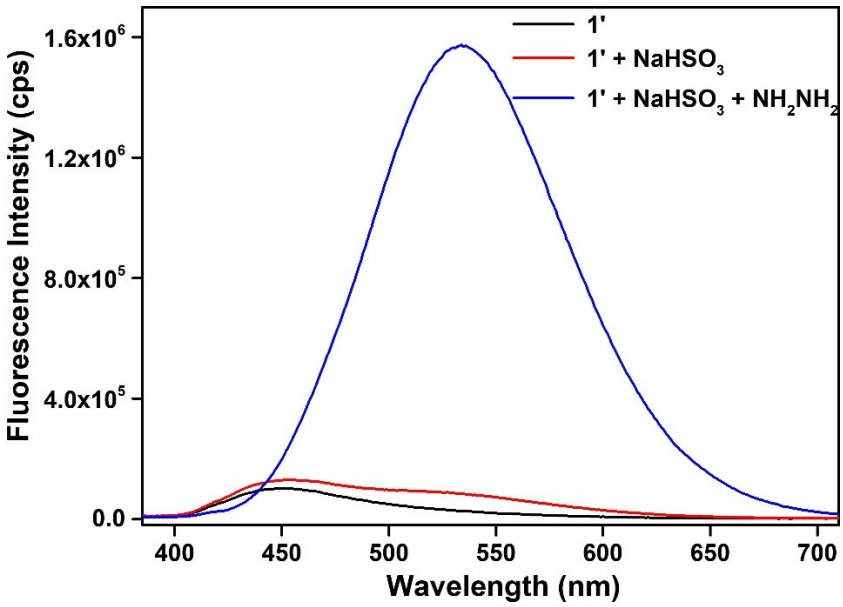

Figure S16. Change in the fluorescence emission intensity of **1′** upon addition of 1 mM hydrazine solution (500 µL) in presence of 1 mM $NaHSO_3$ solution (500 µL).

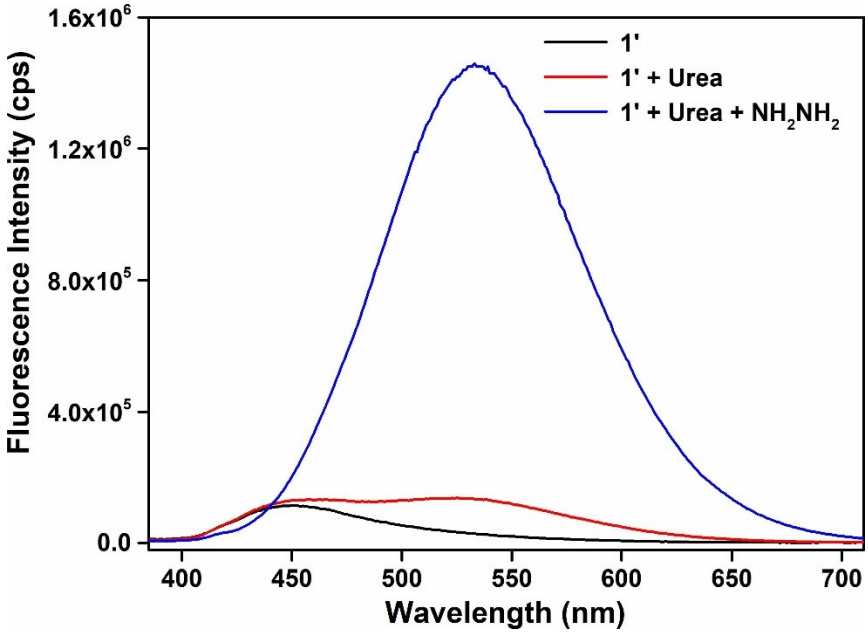

Figure S17. Change in the fluorescence emission intensity of **1′** upon addition of 1 mM hydrazine solution (500 µL) in presence of 1 mM urea solution (500 µL).

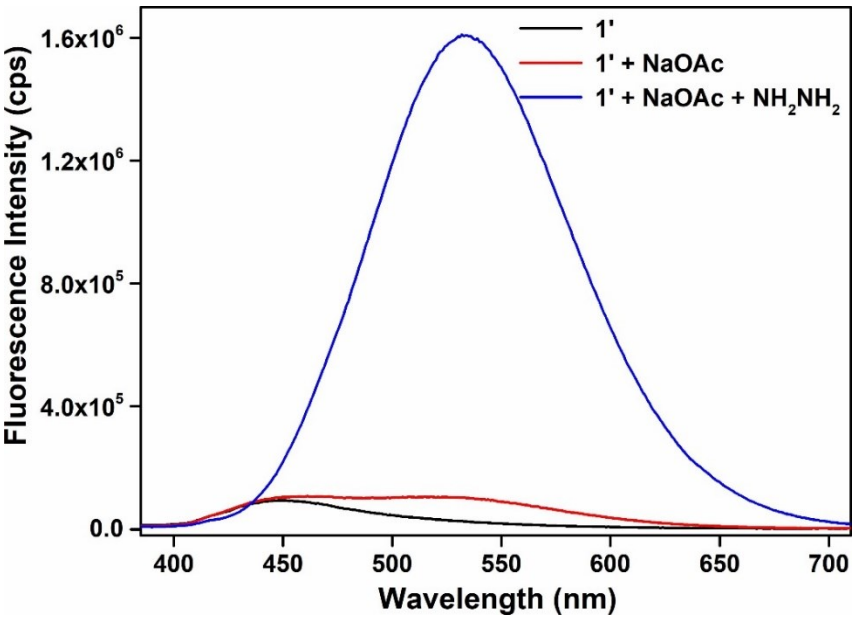

Figure S18. Change in the fluorescence emission intensity of **1′** upon addition of 1 mM hydrazine solution (500 µL) in presence of 1 mM NaOAc solution (500 µL).

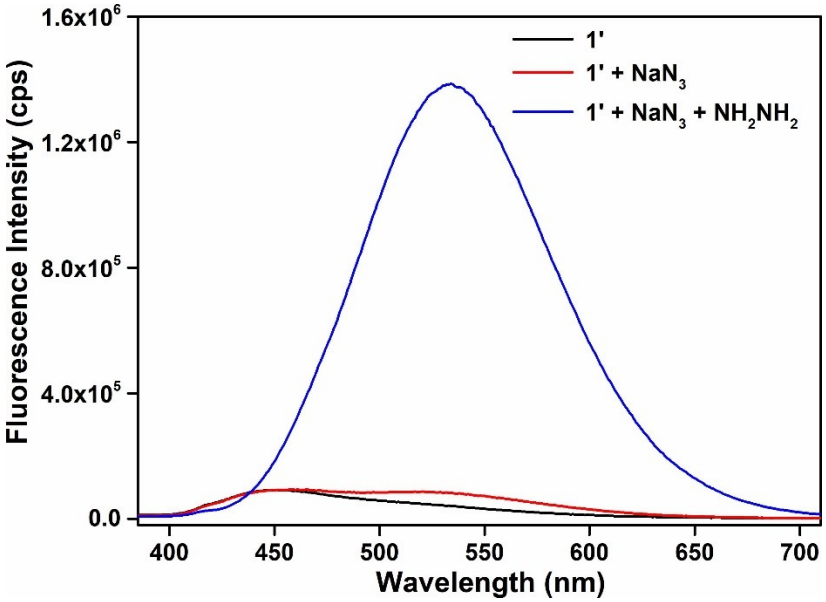

Figure S19. Change in the fluorescence emission intensity of **1′** upon addition of 1 mM hydrazine solution (500 µL) in presence of 1 mM NaN_3 solution (500 µL).

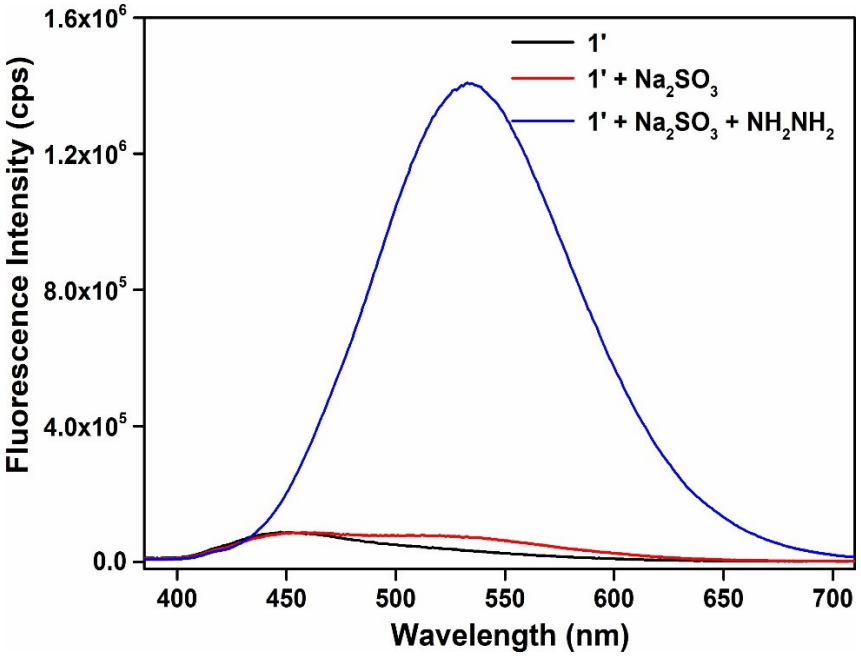

Figure S20. Change in the fluorescence emission intensity of **1′** upon addition of 1 mM hydrazine solution (500 µL) in presence of 1 mM Na_2SO_3 solution (500 µL).

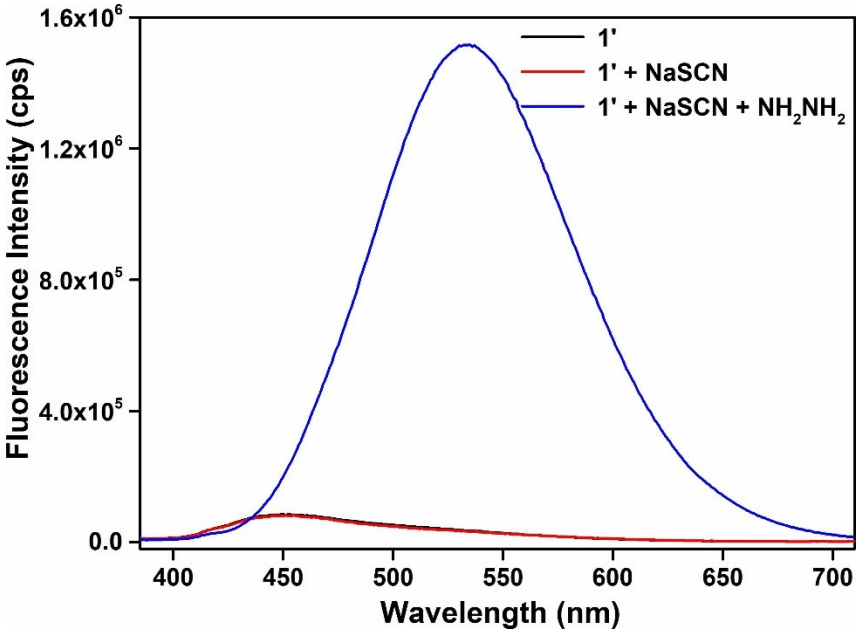

Figure S21. Change in the fluorescence emission intensity of **1′** upon addition of 1 mM hydrazine solution (500 µL) in presence of 1 mM NaSCN solution (500 µL).

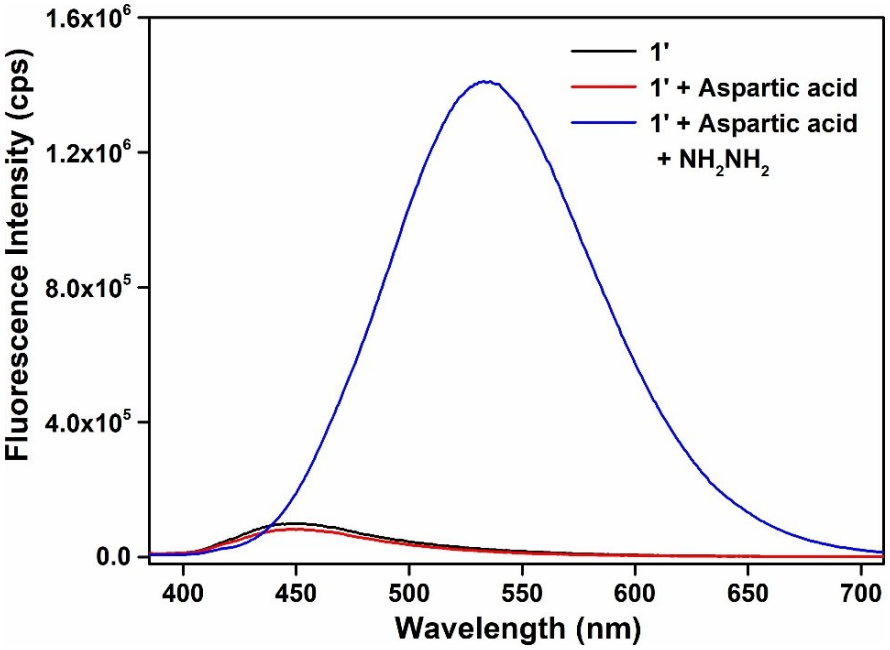

Figure S22. Change in the fluorescence emission intensity of **1′** upon addition of 1 mM hydrazine solution (500 µL) in presence of 1 mM aspartic acid solution (500 µL).

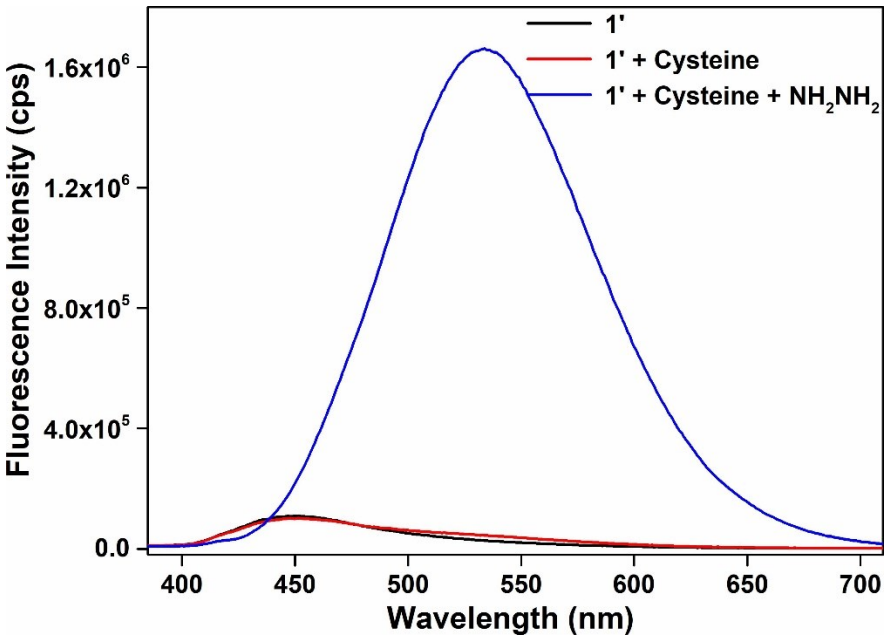

Figure S23. Change in the fluorescence emission intensity of **1′** upon addition of 1 mM hydrazine solution (500 µL) in presence of 1 mM cysteine solution (500 µL).

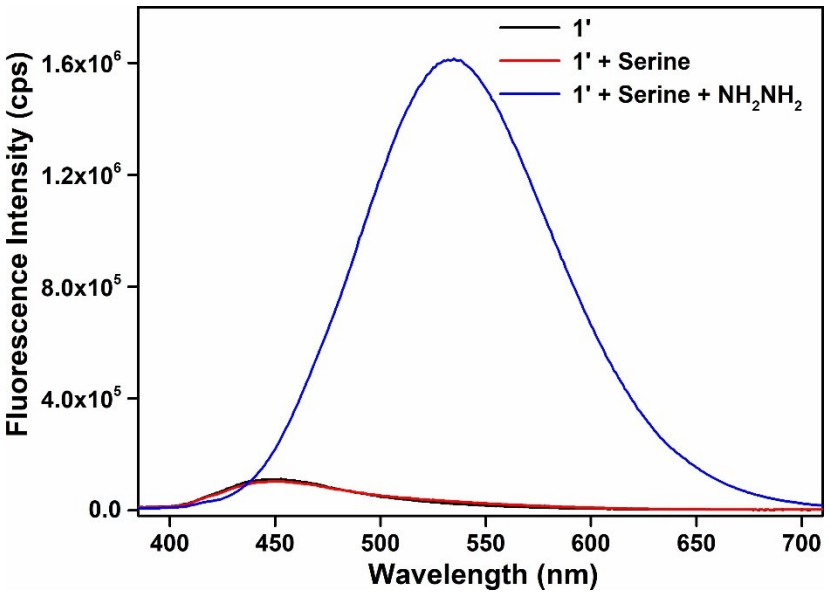

Figure S24. Change in the fluorescence emission intensity of **1′** upon addition of 1 mM hydrazine solution (500 µL) in presence of 1 mM serine solution (500 µL).

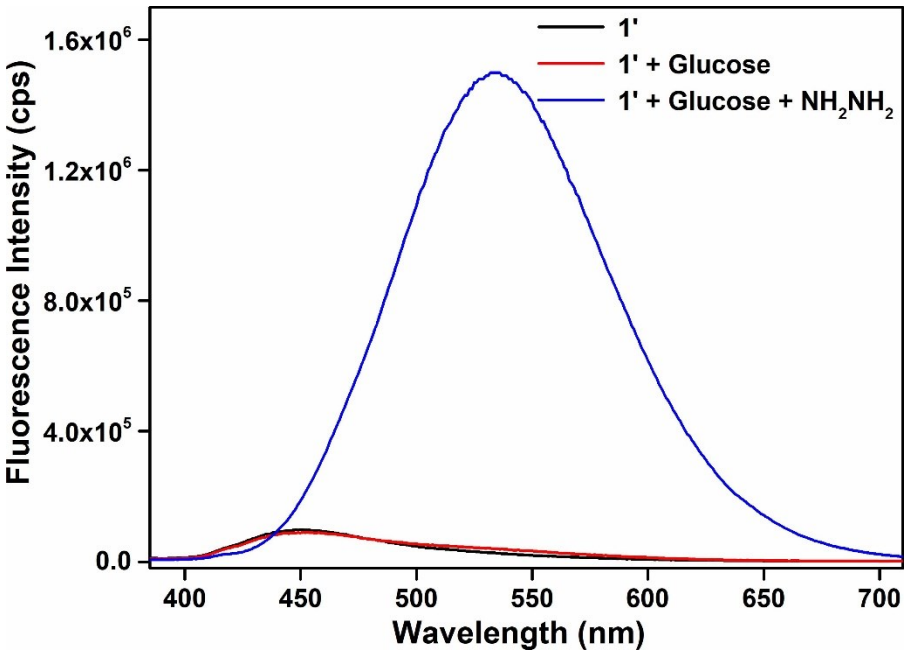

Figure S25. Change in the fluorescence emission intensity of **1′** upon addition of 1 mM hydrazine solution (500 µL) in presence of 1 mM glucose solution (500 µL).

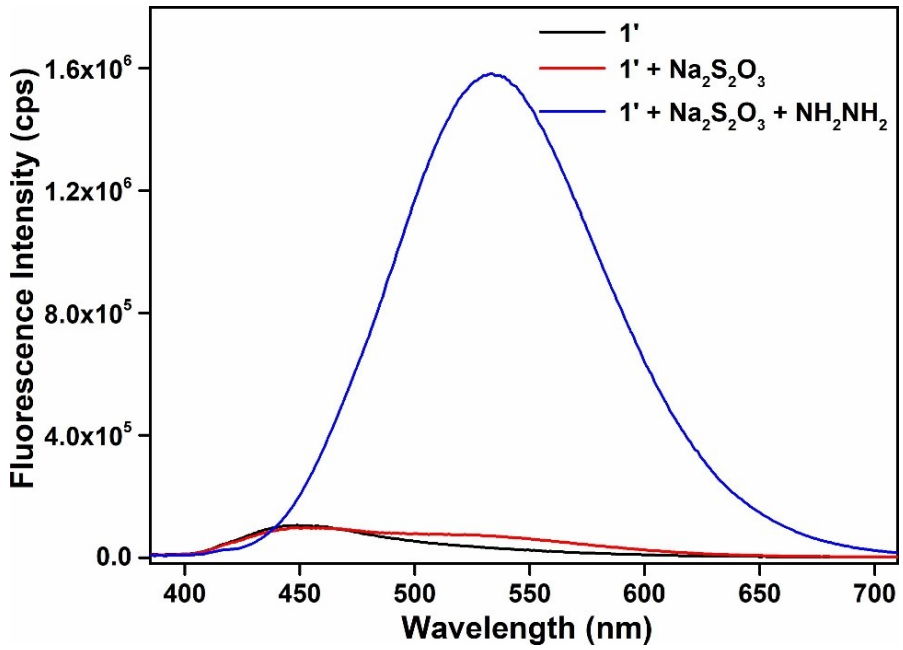

Figure S26. Change in the fluorescence emission intensity of **1′** upon addition of 1 mM hydrazine solution (500 µL) in presence of 1 mM $Na_2S_2O_3$ solution (500 µL).

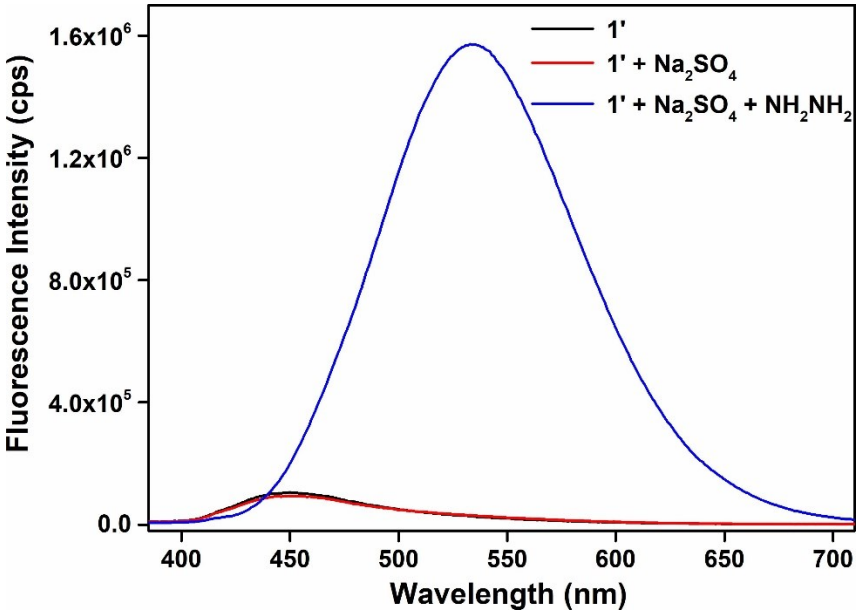

Figure S27. Change in the fluorescence emission intensity of **1′** upon addition of 1 mM hydrazine solution (500 µL) in presence of 1 mM Na_2SO_4 solution (500 µL).

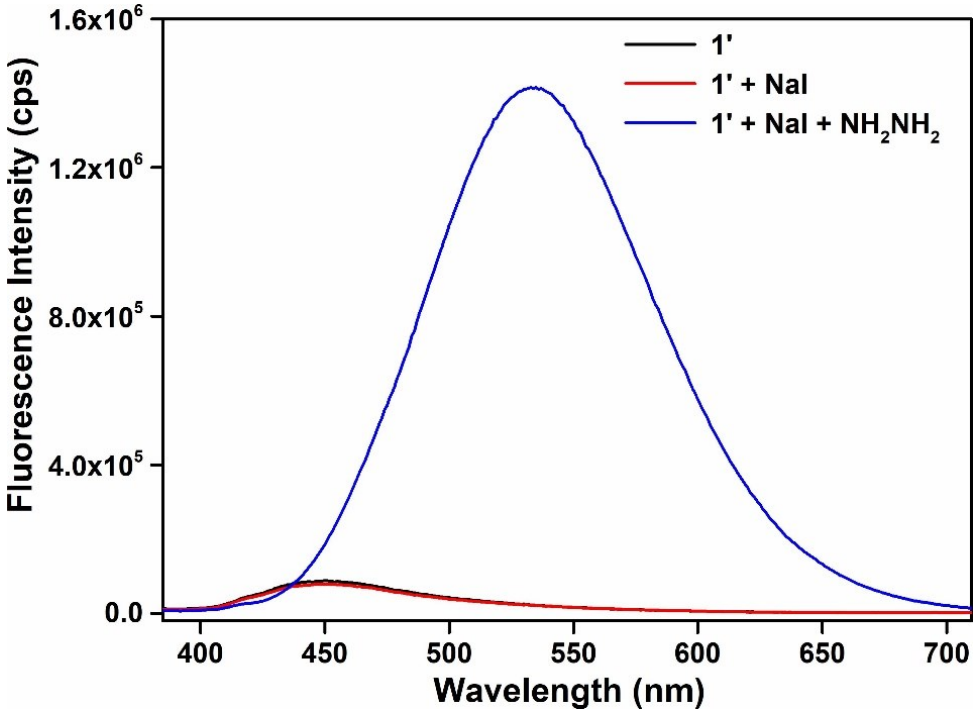

Figure S28. Change in the fluorescence emission intensity of **1′** upon addition of 1 mM hydrazine solution (500 μL) in presence of 1 mM NaI solution (500 μL).

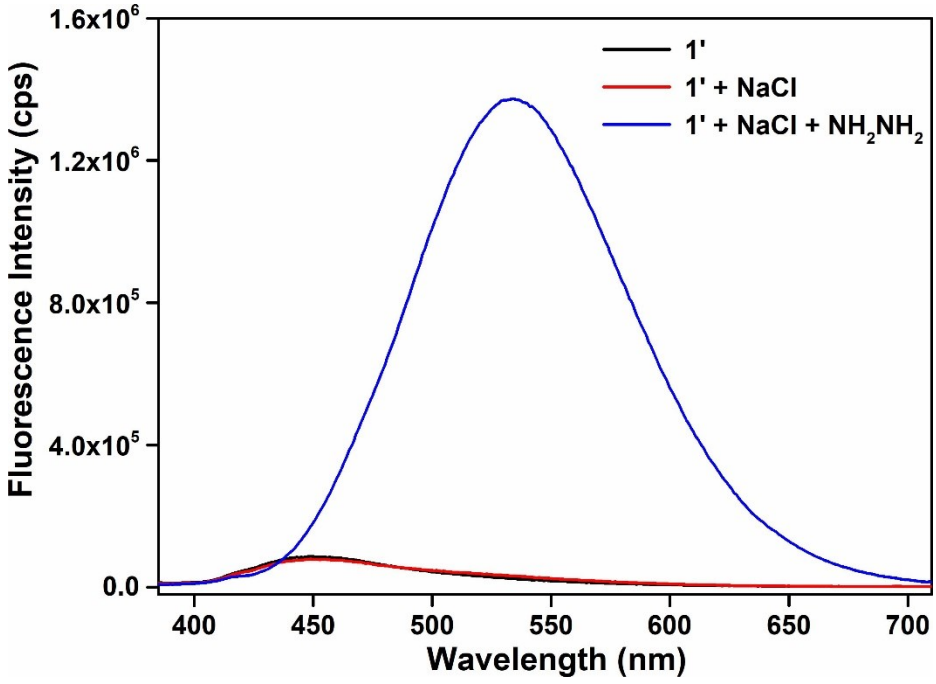

Figure S29. Change in the fluorescence emission intensity of **1′** upon addition of 1 mM hydrazine solution (500 μL) in presence of 1 mM NaCl solution (500 μL).

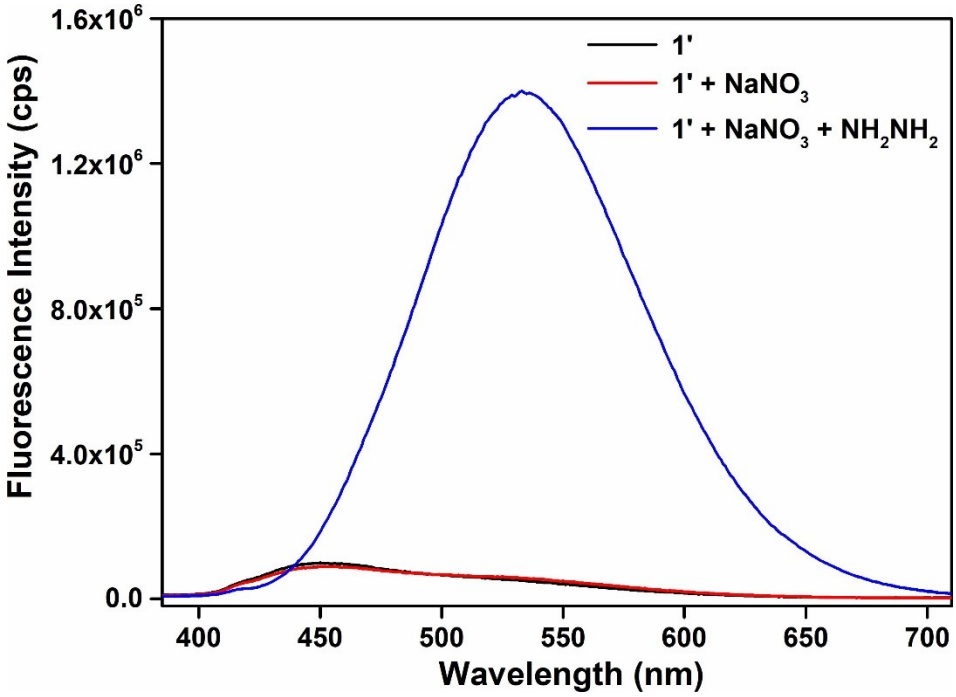

Figure S30. Change in the fluorescence emission intensity of **1′** upon addition of 1 mM hydrazine solution (500 µL) in presence of 1 mM $NaNO_3$ solution (500 µL).

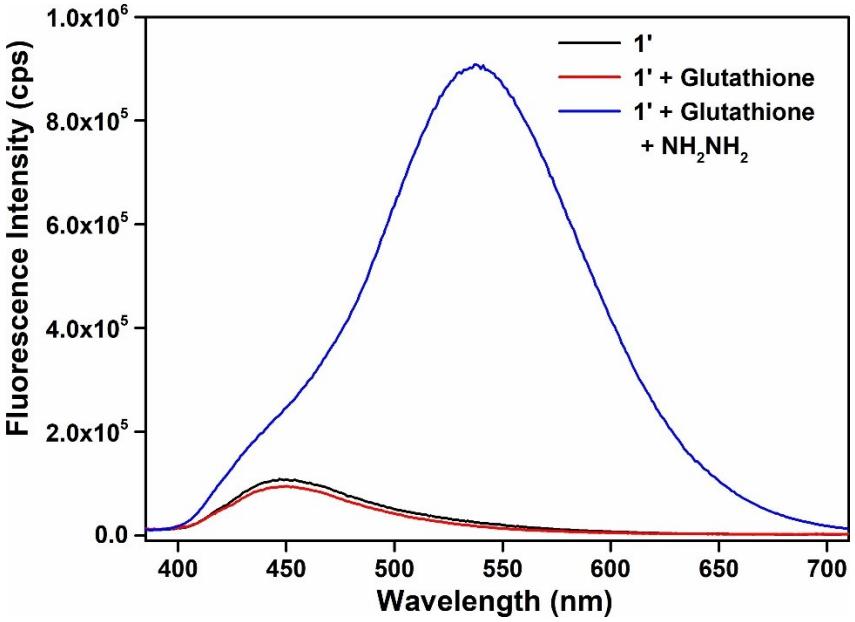

Figure S31. Change in the fluorescence emission intensity of **1′** upon addition of 1 mM hydrazine solution (500 µL) in presence of 1 mM glutathione solution (500 µL).

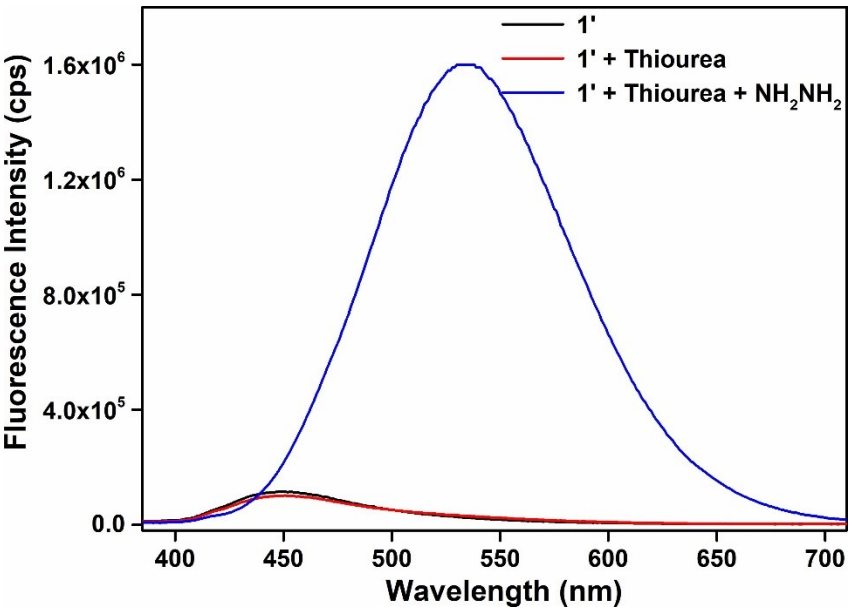

Figure S32. Change in the fluorescence emission intensity of **1′** upon addition of 1 mM hydrazine solution (500 µL) in presence of 1 mM thiourea solution (500 µL).

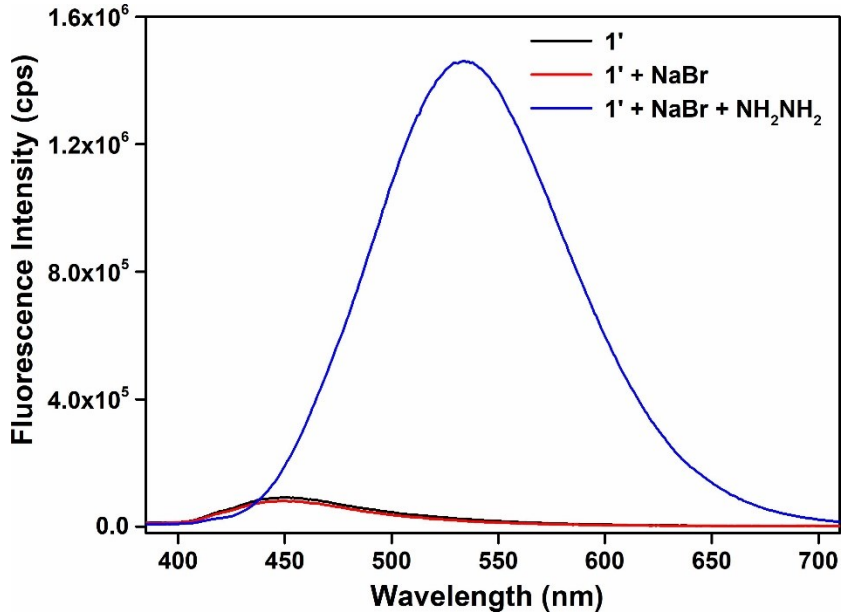

Figure S33. Change in the fluorescence emission intensity of **1′** upon addition of 1 mM hydrazine solution (500 µL) in presence of 1 mM NaBr solution (500 µL).

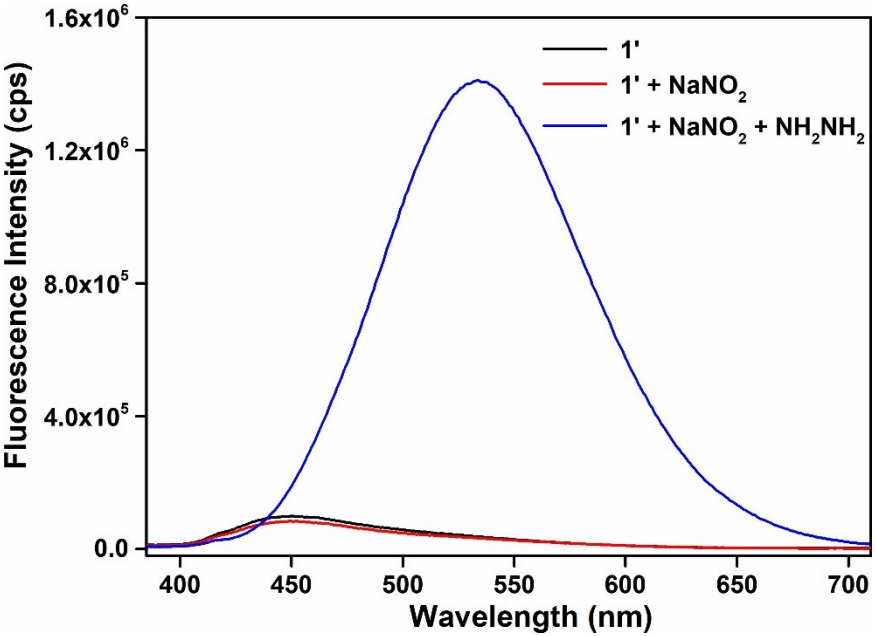

Figure S34. Change in the fluorescence emission intensity of **1′** upon addition of 1 mM hydrazine solution (500 µL) in presence of 1 mM $NaNO_2$ solution (500 µL).

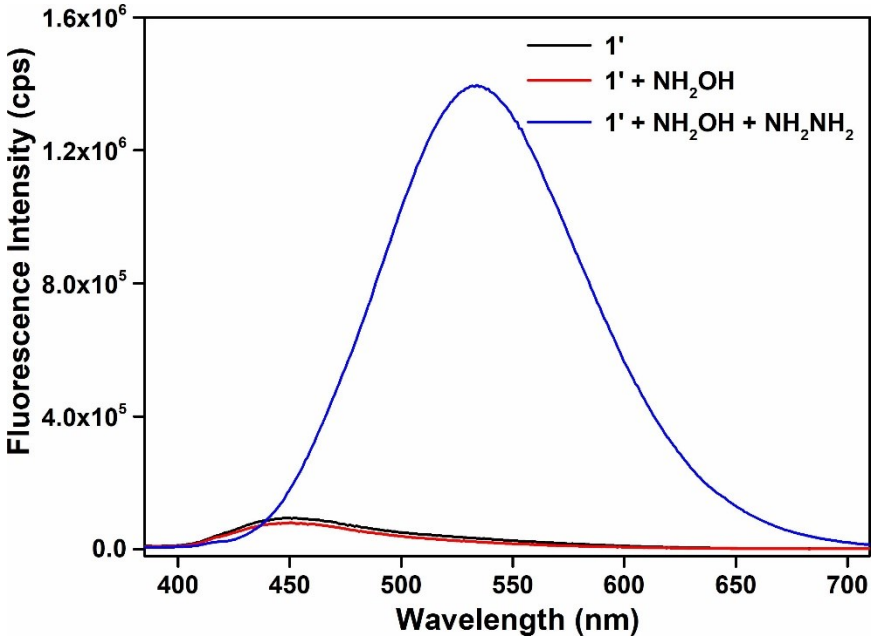

Figure S35. Change in the fluorescence emission intensity of **1′** upon addition of 1 mM hydrazine solution (500 µL) in presence of 1 mM NH_2OH solution (500 µL).

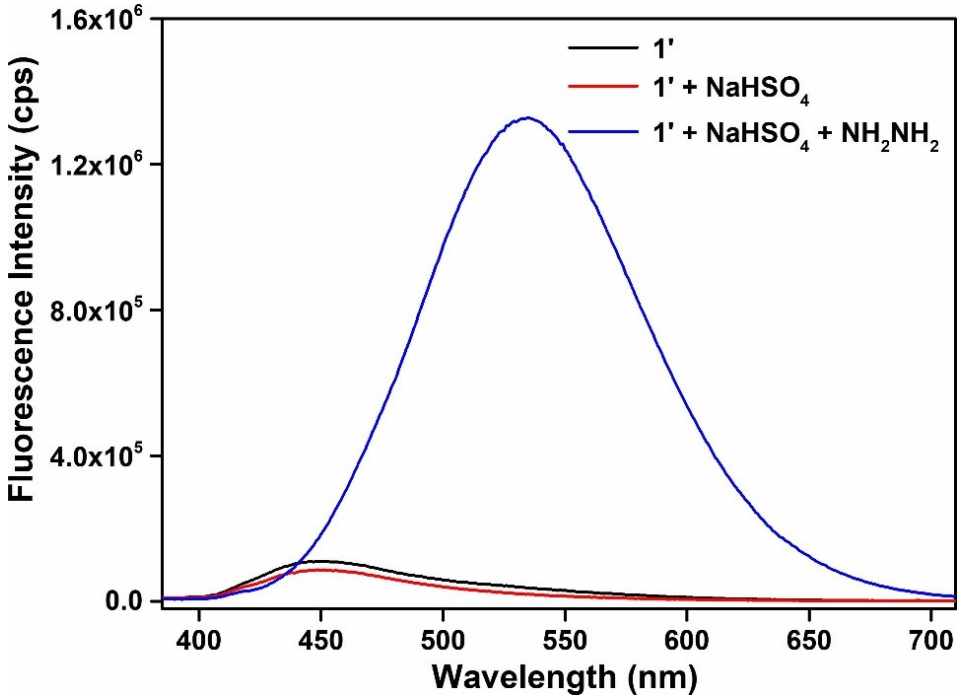

Figure S36. Change in the fluorescence emission intensity of **1′** upon addition of 1 mM hydrazine solution (500 µL) in presence of 1 mM $NaHSO_4$ solution (500 µL).

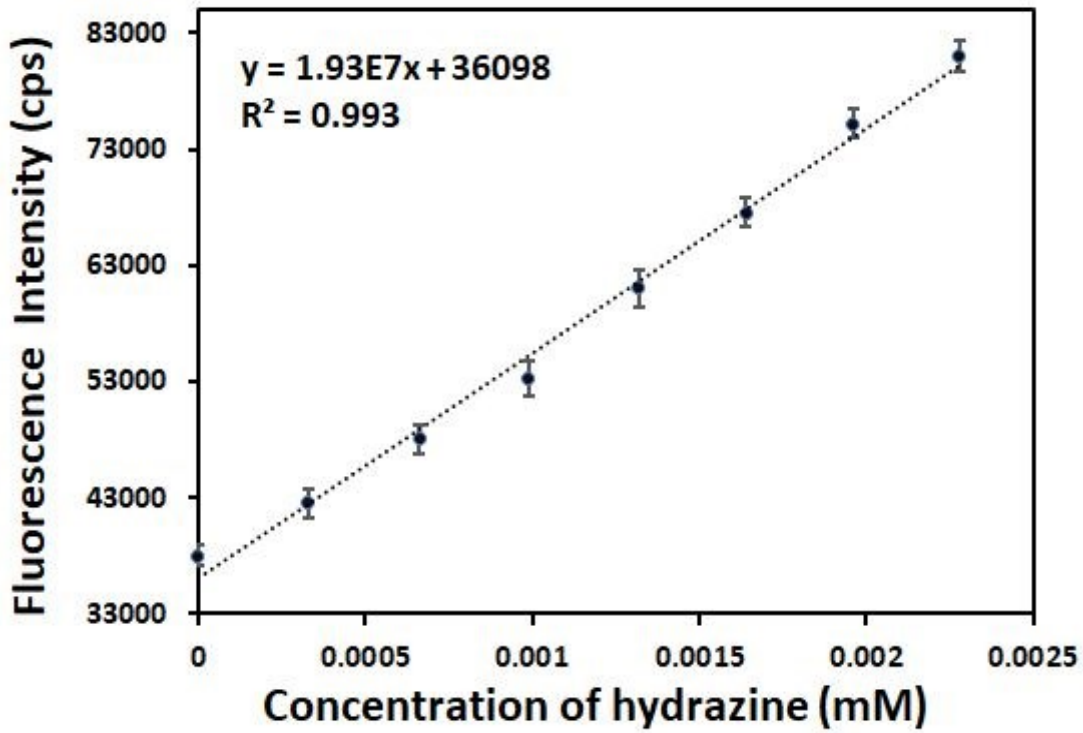

Figure S37. Change in the fluorescence emission intensity of **1′** in aqueous medium as a function of hydrazine concentration. The error bars indicate the standard deviations of three measurements.

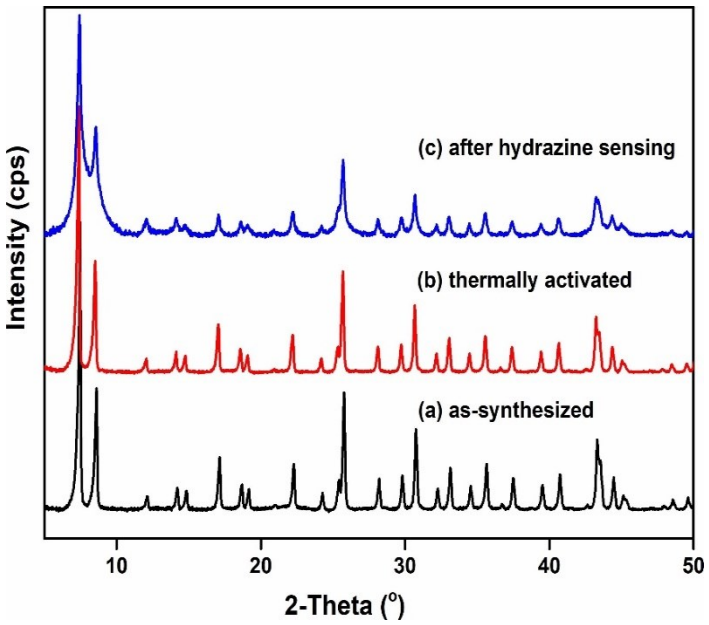

Figure S38. XRPD patterns of **1** in different forms: as-synthesized (a), thermally activated (b) and after hydrazine sensing (c).

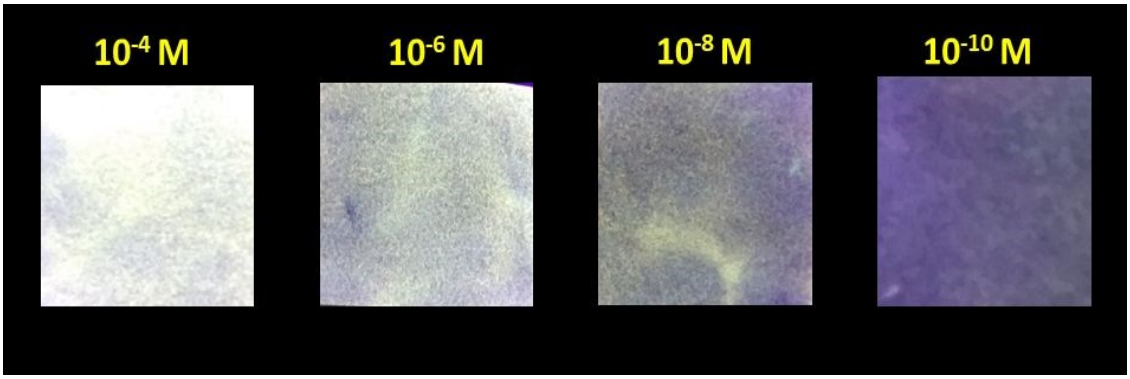

Figure S39. Concentration dependent hydrazine sensing in MOF-coated portable paper strip device.

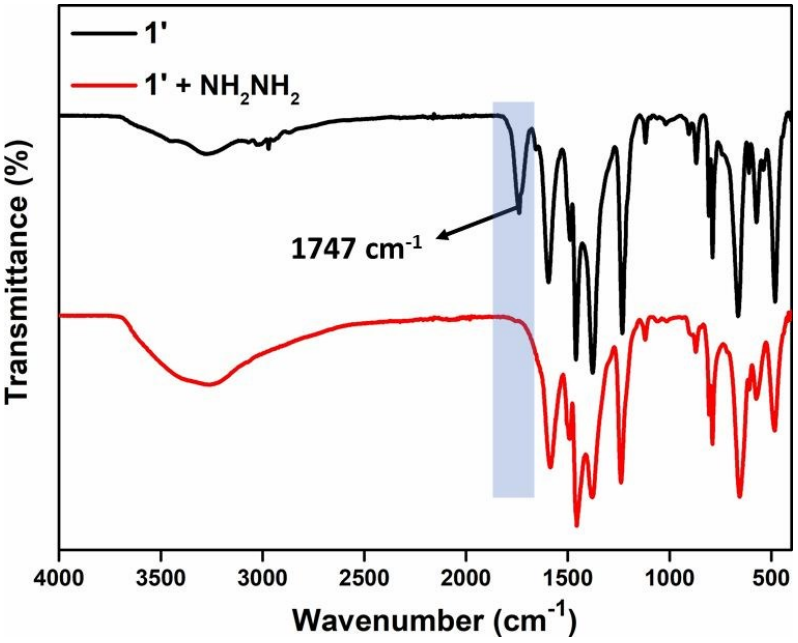

Figure S40. FT-IR spectra of **1′** and hydrazine treated **1′** (recovered after sensing).

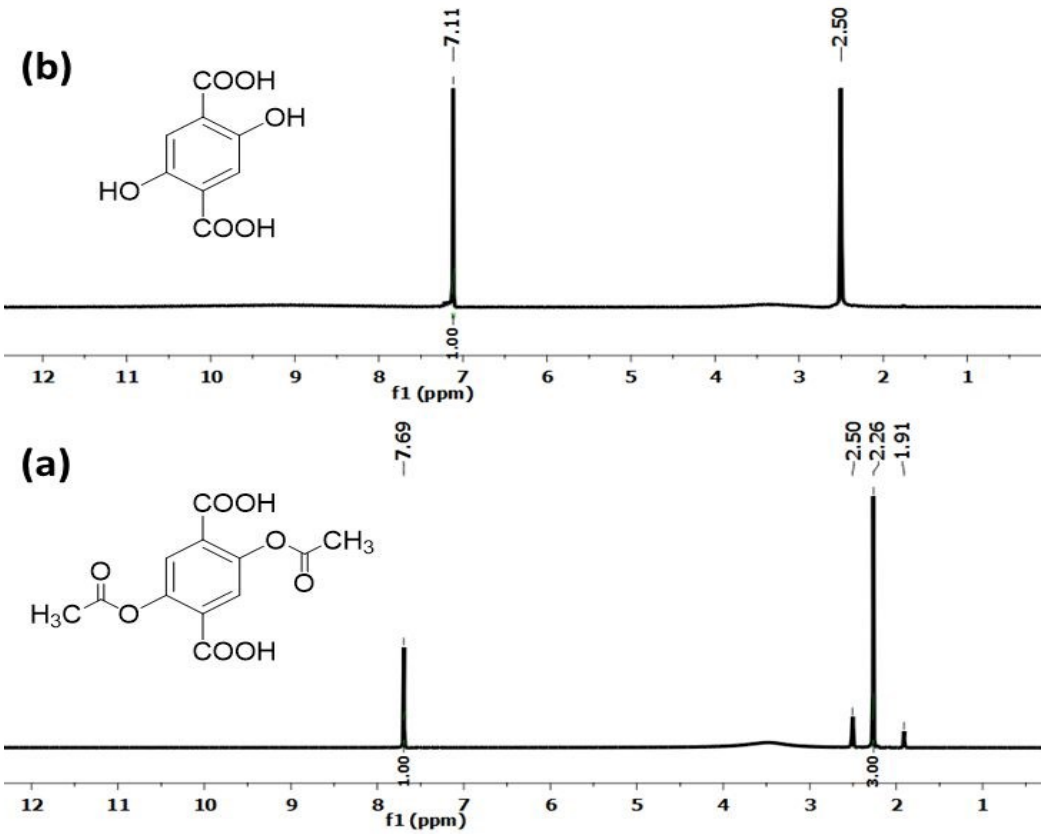

Figure S41. ^{1}H NMR spectrum of (a) $H_2BDC\text{-}(OCOCH_3)_2$ ligand and (b) hydrazine-treated $H_2BDC\text{-}(OCOCH_3)_2$ ligand in DMSO-d_6. Vanishing of signal at 2.26 ppm and up-field shift of aromatic protons from 7.69 ppm to 7.11 ppm signifies the formation of $H_2BDC\text{-}(OH)_2$ after treatment with hydrazine.

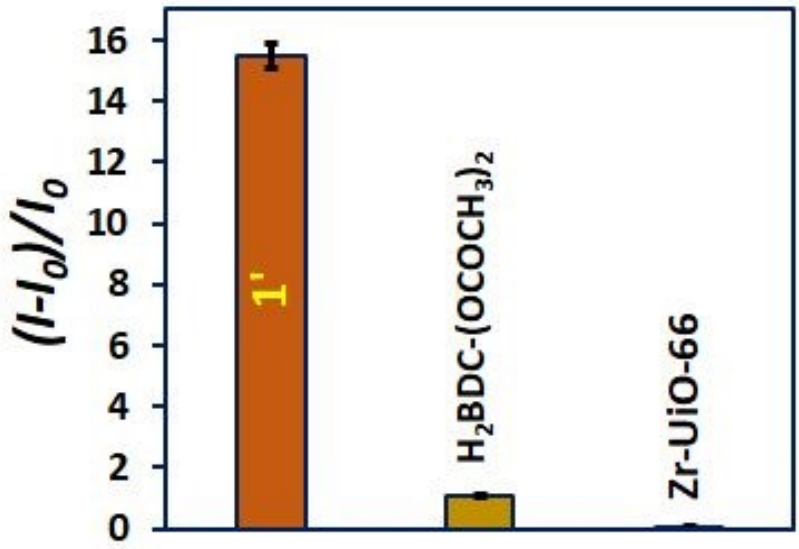

Figure S42. Relative fluorescence response of **1′**, $H_2BDC-(OCOCH_3)_2$ ligand and Zr-UiO-66 towards 1 mM hydrazine (500 µL) in aqueous medium. The error bars indicate the standard deviations of three measurements.

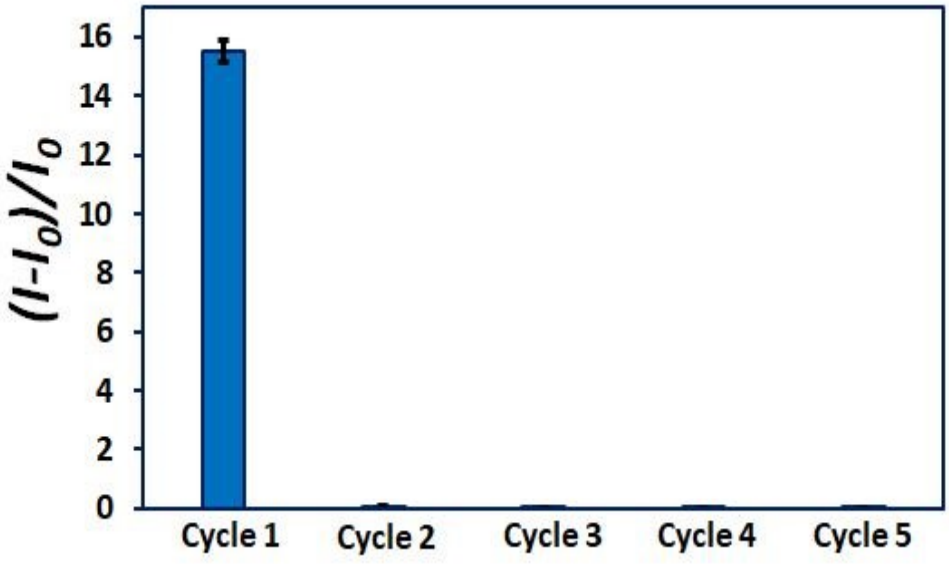

Figure S43. Recyclability test for the fluorescence turn-on response of **1′** towards hydrazine. The error bars indicate the standard deviations of three measurements.

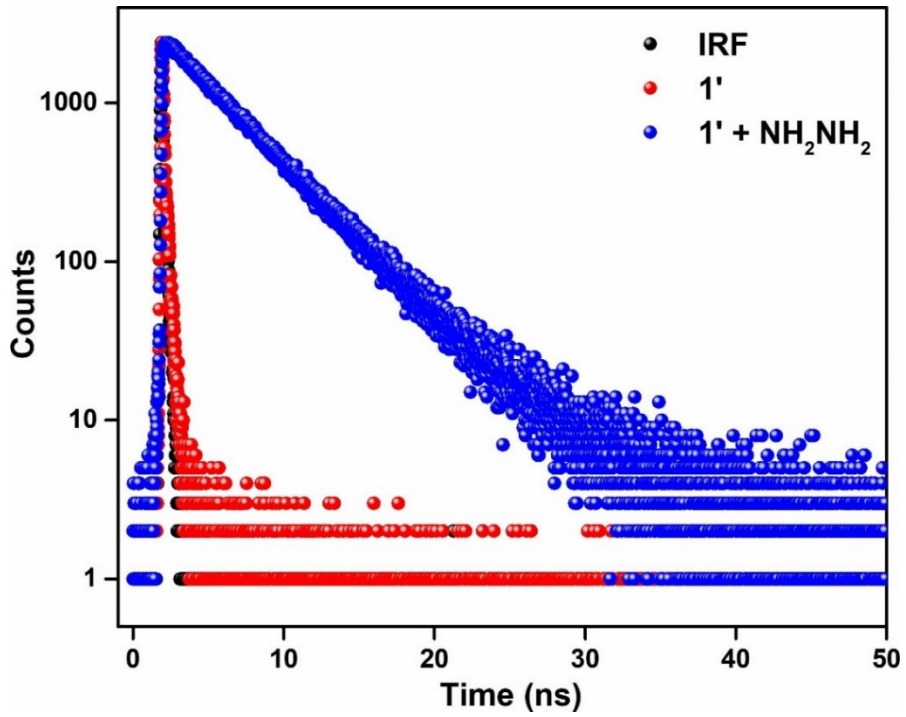

Figure S44. Lifetime decay profiles of aqueous suspension of **1′** in absence and presence of hydrazine solution (λ_{ex} = 375 nm, monitored at 535 nm).

Table S1. Comparison of the sensing performances of various fluorescent sensors of hydrazine.

Sl. No.	Sensor	Type of Material	Sensing Medium	Mode of Detection	Detection Limit	Response Time	Ref.
1	Zr-UiO-66-$(OCOCH_3)_2$	MOF	water	turn-on	78.8 nM	seconds	this work
2	UiO-66-phmd	MOF	HEPES buffer	turn-on	0.87 µM	20 min	4
3	BTI	organic-molecule	HEPES buffer	turn-on	2.9 ppb	20 min	5
4	HyP-1	organic-molecule	PBS buffer	turn-on	0.035 ppb	1 h	6
5	P1	organic-molecule	PBS buffer	turn-on	1.79 nM	40 s	7
6	BPB	BODIPY-based organic	HEPES buffer	turn-off	1.87 µM	-	8

		molecule					
7	Naphsulf-O	organic-molecule	PBS buffer	turn-on	22 nM	40 min	9
8	BBHC	organic-molecule	PBS buffer	turn-on	0.43 μM	1 min	10
9	CFAc	organic-molecule	PBS buffer	ratiometric	0.0474 μM	-	11
10	BI-E	near-infrared fluorescent probe	PBS buffer	turn-on	0.057 μM	1 min	12
11	NA-N_2H_4	naphthalimide based organic molecule	HEPES buffer	ratiometric	9.4 nM	15 min	13
12	TAPHP	organic-molecule	HEPES buffer	ratiometric	0.3 μM	60 min	14
13	AB-NDI	organic-molecule	DMSO	turn-on	-	-	15
14	TNQ	organic-molecule	PBS buffer	ratiometric	-	-	16
15	HBTM	organic-molecule	PBS buffer	turn-on	29 μM	55 min	17
16	NAC	naphthalene based organic molecule	HEPES buffer	turn-on	4.5 μM	4 min	18
17	DPA	organic-molecule	DMSO/ PBS buffer solution (4/6, v/v)	turn-on	1.9 nM	8 min	19
18	probe **1** probe **2**	pyrene- and anthracene-based organic molecule	HEPES buffer	turn-on	0.17 μM 0.24 μM	3 min	20
19	SF-Azo compounds	organic-molecule	CH_3OH/ H_2O (v/v	turn-on	2.33 mM	18-42 min	21

			= 1:1)				
20	levulinated hydroxy-coumarin 1	organic-molecule	acetate buffer	turn-on	2.46 μM	15 min	22
21	Compound **6a**	organic-molecule	HEPES/ DMSO (1:1, v/v)	"turn-on" and "ratiomet-ric"	0.19 μM	-	23
22	NS-N_2H_4	organic-molecule	PBS/ DMSO (v/v = 2/1)	turn-on	-	240 min	24
23	PBF	organic-molecule	CH_3CN–H_2O (6: 4, v/v),	turn-on	0.41 μM	1 min	25

Table S2. Unit cell parameters of the as-synthesized Zr-UiO-66-$(OCOCH_3)_2$ MOF. The obtained values are compared with the previously reported Zr-UiO-66 MOFs.

Compound Name	Zr-UiO-66-$(OCOCH_3)_2$ MOF (**1′**) (this work)	Zr-UiO-66 MOF (reported)[26]	Zr-UiO-66-NH-CH_2-Py MOF (reported)[27]	Zr-UiO-66-1-(aminomethyl) naphthalen-2-ol (reported)[28]
Crystal System	cubic	cubic	cubic	cubic
a = b = c (Å)	20.840(7)	20.7004 (2)	20.755(3)	20.786(3)
α = β= γ (°)	90	90	90	90
V (Å^3)	9051.7(5)	8870.3(2)	8940.3(21)	8981.1(19)

Table S3. Calculation of detection limit for hydrazine detection by **1′**.

Number of Run (n)	Fluorescence Intensities at 535 nm before addition of hydrazine	Standard Deviation (σ)	Slope (k) (mM^{-1})	Detection Limit ($3\sigma/k$) (mM)
1	37276.92401	509.41	19374748	7.88×10^{-5} (78.8 nM) (3.9 ppb)
2	38905.85504			
3	38773.16733			
4	39000.68352			
5	38704.43693			
6	38620.54759			
7	38774.00126			
8	38635.82115			

Table S4. Fluorescence lifetimes of aqueous suspension of **1′** before and after the addition of hydrazine solution (λ_{ex} = 375 nm, pulsed diode laser).

Volume of 1 mM NH_2NH_2 solution added (μL)	a_1	a_2	τ_1 (ns)	τ_2 (ns)	$<\tau>$* (ns)	χ^2
0	0.64	0.36	0.08	0.31	0.16	1.06
500	0.96	0.04	4.33	8.88	4.47	1.12

* $<\tau> = a_1\tau_1 + a_2\tau_2$

References

1. J. Liu, Y. Xu, P. B. Groszewicz, M. Brodrecht, C. Fasel, K. Hofmann, X. Tan, T. Gutmann and G. Buntkowsky, *Catal. Sci. Technol.*, 2018, **8**, 5190-5200.
2. A. Boultif and D. J. Louer, *J. Appl. Crystallogr.*, 1991, **24**, 987-993.
3. Stoe and C. GmbH, STOE WinXPOW version 2.11, Darmstadt, Germany, 2005.
4. M. SK, M. R. U. Z. Khan, A. Das, S. Nandi, V. TrivedI and S. Biswas, *Dalton Trans.*, 2019, **48**, 12615-12621.
5. R. Maji, A. K. Mahapatra, K. Maiti, S. Mondal, S. S. Ali, P. Sahoo, S. Mandal, M. R. Uddin, S. Goswami, C. K. Quah and H.-K. Fun, *RSC Adv.*, 2016, **6**, 70855-70862.
6. Y. Jung, I. G. Ju, Y. H. Choe, Y. Kim, S. Park, Y.-M. Hyun, M. S. Oh and D. Kim, *ACS Sens.*, 2019, **4**, 441-449.
7. Shweta, A. Kumar, Neeraj, S. K. Asthana, A. Prakash, J. K. Roy, I. Tiwari and K. K. Upadhyay, *RSC Adv.*, 2016, **6**, 94959-99496.

8. A. K. Mahapatra, R. Maji, K. Maiti, S. K. Manna, S. Mondal, S. S. Ali, S. Manna, P. Sahoo, S. Mandal, M. R. Uddin and D. Mandal, *RSC Adv.*, 2015, **5**, 58228-58236.
9. W. Chen, W. Liu, X.-J. Liu, Y.-Q. Kuang, R.-Q. Yu and J.-H. Jiang, *Talanta*, 2017, **162**, 225-231.
10. S. Paul, R. Nandi, K. Ghoshal, M. Bhattacharyya and D. K. Maiti, *New J. Chem.*, 2019, **43**, 3303-3330.
11. Z. Zhang, Z. Zhuang, L. L. Song, X. Lin, S. Zhang, G. Zheng and F. Zhan, *J. Photochem. Photobiol. A*, 2018, **358**, 10-16.
12. J. Ma, J. Fan, H. Li, Q. Yao, J. Xia, J. Wang and X. Peng, *Dyes Pigm.*, 2017, **138**, 39-46.
13. X. Xia, F. Zeng, P. Zhang, J. Lyu, Y. Huang and S. Wu, *Sens. Actuators, B*, 2017, **227**, 411-418.
14. Z. Luo, B. Liu, T. Qin, K. Zhu, C. Zhao, C. Pan and L. Eang, *Sens. Actuators, B*, 2018, **263**, 229-236.
15. D. Zhou, Y. Wang, J. Jia, W. Yu, B. Qu, X. Li and X. Sun, *Chem. Commun.*, 2015, **51**, 10656-10659.
16. S. Yu, S. Wang, H. Yu, Y. Feng, S. Zhang, M. Zhu, H. Yin and X. Meng, *Sens. Actuators, B*, 2015, **220**, 1338-1345.
17. Z. Chen, X. Zhong, W. Qu, T. Shi, H. Liu, H. He, X. Zhang and S. Wang, *Tetrahedron Lett.*, 2017, **58**, 2596-2601.
18. S. Goswami, A. K. Das, U. Saha, S. Maity, K. Khanra and N. Bhattacharyya, *Org. Biomol. Chem.*, 2015, **13**, 2134-2139.
19. Y. Zhang, Y. Huang, Y. Yue, J. Chao, F. Huo and C. Yin, *Sens. Actuators, B*, 2018, **273**, 944-950.
20. B. Roy, S. Halder, A. Guha and S. Bandyopadhyay, *Anal. Chem.*, 2017, **89**, 10625-10636.
21. M. C. Shin, Y. Lee, S. B. Park and E. Kim, *ACS Omega*, 2019, **4**, 14875-14885.
22. M. G. Choi, J. Hwang, J. O. Moon, J. Sung and S.-K. Chang, *Org. Lett.*, 2011, **13**, 5260-5263.
23. D. Purohit, C. P. Sharma, A. Raghuvanshi, A. Jain, K. S.Rawat, N. M.Gupta, J. Singh, M. Sachdev and A. Goel, *Chem. Eur.J.*, 2019, **25**, 4660-4664.
24. J.-Y. Wang, Z.-R. Liu, M. Ren and W. Lin, *Sci. Rep.*, 2017, **7**, 1-8.
25. S. Goswami, S. Paul and A. Manna, *New J. Chem.*, 2015, **39**, 2300-2305.
26. J. H. Cavka, S. Jakobsen, U. Olsbye, N. Guillou, C. Lamberti, S. Bordiga and K. P. Lillerud, *J. Am. Chem. Soc.*, 2008, **130**, 13850-13851.
27. A. Das, N. Anbu, M. SK, A. Dhakshinamoorthy and S. Biswas, *Dalton Trans.*, 2019, **48**, 17371-17380.
28. A. Das, N. Anbu, M. SK, A. Dhakshinamoorthy and S. Biswas, *ChemCatChem*, 2020, **12**, 1789-1798.